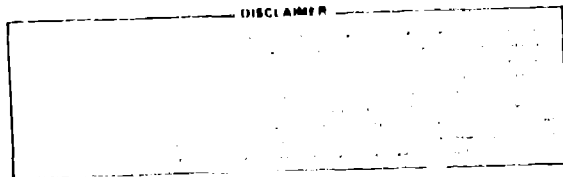**LA-UR**-82-566

Conf-811229--10

LA-UR--82-566

DE82 011972

TITLE. ULTRAVIOLET PHASE CONJUGATION

MASTER

AUTHOR(S): M. Slatkine, AP-5
Irving J. Bigio, AP-5
Robert A. Fisher, AP-5
M. L. Maloney, AP-5
J. R. Busse, AP-5
R. G. Tercovich, AP-5
B. J. Feldman, AP-5

SUBMITTED TO. International Conference on Lasers '81
New Orleans, Louisiana, Dec. 14-18, 1981

Los Alamos
Los Alamos National Laboratory
Los Alamos, New Mexico 87545

ULTRAVIOLET PHASE CONJUGATION

M. Slatkine, Irving J. Bigio, Robert A. Fisner, M. L. Maloney,
J. R. Busse, R. G. Tercovich and B. J. Feldman
University of California
Los Alamos National Laboratory
Los Alamos, New Mexico 87545

Abstract

Diffraction-limited phase conjugate reflection of an injection-locked high-power
(~ 1 MW) ultraviolet excimer laser beam has been demonstrated via stimulated Brillouin
scattering. Reflectivities higher than 70% were attained. Limitations as well as
coherence and power requirements for image retention are discussed.

Introduction

Considerable attention has been given recently to phase-conjugate reflection [1] of
ultraviolet laser beams [2]. Potential applications, among others, are in laser fusion
and in high resolution photolithography [3]. Phase conjugation in the ultraviolet was
first reported using a quadrupled Nd:YAG (λ = 2660 Å) laser [2]. Reflectivities
below 0.1% were obtained by degenerate four-wave mixing in several liquids. Since
excimer lasers are the most powerful ultraviolet radiation sources available today, much
effort has been made to reverse their wavefront. The successful development of simple
injection-locking techniques in conjunction with these fast (~ 20 ns) pulsed laser
sources has paved the way to the successful wavefront reversal of excimer laser beams.
Two approaches have been (and are still being) investigated: (a) degenerate four-wave
mixing, particularly via the production of thermal gratings [6,7]; (b) wavefront reversal
via stimulated Brillouin backward scattering (SBBS).

Although four-wave mixing seems to have some inherent advantages as to the ability of
reversing highly aberrated beams, it is not yet clear which approach is more practically
efficient with the high power excimer lasers. We have followed both approaches [7,8].
In this paper we shall emphasize the SBBS approach. It is the purpose of the present
paper to describe some experiments which have led to efficient (70% reflection) wavefront
reversal of an excimer high-power (> 1 MW) ultraviolet laser beam. We shall elucidate
the physical principles involved with SBBS in terms of diffraction from density
gratings. In addition, we shall compare the process to four-wave mixing.

Degenerate Four-Wave Mixing and SBBS

Degenerate Four-Wave Mixing

In this section we briefly describe the four-wave mixing process (Fig. 1a). It will
later serve us to understand SBBS. The experimental setup consists of two precisely
counterpropagating pump beams (p_1 and p_2) and a probe beam. The probe beam is usually
much weaker than the pump beam and is to be phase conjugated. Pump p_1 and the probe
beam interfere to set up an intensity grating which generates a material grating through
the interaction between the optical field and the material. The second pump beam p_2 is
diffracted (Bragg reflection) from the material grating to appear as the phase conjugated
probe beam. The reflectivity of each Bragg plane depends upon the nonlinear suscepti-
bility of the material and the pump's intensities. There is a typical minimum number of
Bragg planes and consequently a minimum grating depth L_{min} [1] required for an
efficient (100%) four-wave mixing phase conjugate reflection. This minimum length, which
depends upon the reflectivity of each Bragg plane, determines the coherence requirements
from the laser in the "real-time holography" experiment.

To understand the power requirements for the phase conjugation of a highly aberrated
beam, one decomposes the probe beam into a set of plane waves (Fig. 1b). Each plane wave
interferes with the pump beams to produce its own grating. The power requirements for a
single grating reflection multiplied by the number of plane waves (which depends upon the
degree of aberration) will give the power requirement for wavefront reversal of an
aberrated beam.

Stimulated Backward Brillouin Scattering (SBBS)

Stimulated backward Brillouin scattering has been extensively investigated in the past, although mainly not in conjunction with phase conjugation. The first demonstration of the effect dates back to 1964 [9]. The use of SBBS for phase conjugation has been first demonstrated by Zel'dovich in 1972 [10] and consequently in the visible and near ir parts of the spectrum by several groups [1 and references there]. In all cases highly coherent pulsed lasers (Ruby, Nd:YAG) have been used.

In this paragraph we elucidate the physical principles behind SBBS in a simple qualitative way which, however, provides an understanding of requirements and limitations for the wavefront reversal of aberrated beams. Rather complex quantitative mathematical analysis can be found in the literature. Figures 2a - 2c outline the relevant physical effects.

Figure 2a shows the Brillouin reflection of a coherent optical beam from an acoustic ultrasonic wave. The acoustic wave of wavelength λ_s, frequency ω_s and velocity v_s ($v_s = \omega_s \lambda_s / 2\pi$) forms a moving grating. An optical beam of wavelength λ_0 ($\sim \lambda_s$) incident on the acoustic wave at the Bragg angle θ_B ($2\lambda_s \cos \theta_B = m\lambda_0$, m - integer) will experience a mirror reflection through positive interference and a Doppler frequency shift. The frequency shift will be ω_s.

Angular Resolution. The acceptance angle of the grating (angles fulfilling Bragg conditions for positive interference) will be $\theta_B \pm \delta\theta$, where $\delta\theta \sim 1/\sqrt{N}$, N being the number of Bragg planes. The angular resolution of the grating will thus be $\sim 1/\sqrt{N}$ (notice: for a given grating and a given incident beam, there will be a single well-defined reflection angle. For a given incident beam and a given reflection angle, there will be many N-Bragg-planes ratings fulfilling the Bragg condition. The angular separation between these gratings will be up to $\delta\theta \sim 1/\sqrt{N}$).

Figure 2b depicts the way by which optical radiation can interact with transparent matter to produce an intensity grating. Since electrical dipoles interact with the gradient of an electric field, and optical intensity gradient (∇I) will induce a material density gradient. An analysis of this effect (electrostriction) shows that the effective mechanical pressures involved are closely equal to the radiation pressure of a "photon gas" I/c, c = light velocity.

Figure 2c elucidates the amplification process of a weak optical beam (frequency ω) precisely counterpropagating a strong beam (frequency ω_0, $\omega-\omega_0=\omega_s<<\omega_0$), via Brillouin scattering in a transparent material. The two counterpropagating beams interfere to produce a moving intensity grating of plane separation $\lambda_0/2$. If ω_s equals the sound frequency for an acoustic wavelength $\lambda_s=\lambda_0/2$, the system will resonate to produce a moving density grating (acoustic wave). The strong beam will be backward reflected (Bragg reflection) from the acoustic wave and frequency shifted just to beat with the incident beam and to enhance the acoustic wave. The net result of this positive feedback is the amplification of the weak beam and the disappearance of the strong beam. The gain at each point is proportional to the incident beam's intensity I. To observe a net gain, the amplification process has to compete with losses due to viscosity (acoustic wave decay) and to optical absorption.

SBBS. A coherent optical beam of high enough intensity can be backward-reflected (phase conjugated) and frequency shifted while impinging on a passive transparent material. This is achieved via Brillouin scattering. Referring again to Fig. 2c, weak optical beams at frequency $\omega_s=\omega_s$ are always present as zero point fluctuations. The backward amplification process through interference with the intense beam at frequency ω_0, described above, can be applied to the noisy beams. For an input beam of intensity I above some threshold intensity I_{th} (in liquids, $I_{th} \sim 1$ GW/cm^2, depending upon the viscosity and optical absorption in the passive material), a noisy beam counterpropagating the input beam will experience a net amplification, thus causing the appearance of a stimulated backward scattered beam. In this process, a stimulated acoustic wave is also being produced. The number N of stimulated Bragg planes responsible for an efficient ($\sim 100\%$) backward reflection of the input beam will determine the angular inaccuracy $\delta\theta$ ($\delta\theta \sim 1/\sqrt{N}$) of the stimulated phase conjugation. The angular accuracy of SBBS, which stems from the fact that the stimulated acoustic waves and the scattering process start from noise is in contrast to the angular accuracy of phase conjugate reflection in four-wave mixing where the diffraction gratings are being produced from well prealigned beams. (For probe beams brighter than zero point fluctuations, i.e., high enough signal noise ratio.)

SBBS of a Focused Coherent Beam

SBBS can be achieved by focusing a coherent beam of intensity I into a transparent material. See Fig. 3a. By using a lens of small enough f_{No} ($f_{No} \equiv f/D$ = focal length/diameter), the threshold intensity for SBBS can be attained at the focal region which is of diameter $\lambda_0 F_{No}$. We list and explain several requirements for achieving a good quality phase conjugate reflection of a focused beam:

a. $f_{No} \leq \sqrt{I/I_{th}\lambda_0^2}$ (For threshold intensity at the focal region.)

b. The angular divergence of the stimulated backward reflected beam at the focal region may be D/f for diffraction-limited recollimation by the lens of diameter D. This requires the utilization of $N = (f/D)^2$ stimulated Bragg planes for the stimulated backward reflection, and consequently the entire focal region. Since the reflectivity R of each Bragg plane at threshold is a well-defined quantity determined by the materials properties, the focal region should not be longer than $\sim \lambda_0/R$; we thus also require

$f_{No} \leq \sqrt{1/R}$.

For each transparent material we thus have a maximum f_{No}, independent of intensity, above which no diffraction limited SBBS is possible.

c. The coherence length ℓ_c required from the laser being used in SBBS is $\ell_c >$ focal length region:

$$\ell_c > \frac{\lambda_0}{r} \cdot \frac{I}{I_{th}\lambda_0}$$

Image Retention in SBBS

To analyze the laser power requirements for high quality image retention of a phase conjugated beam via SBBS, one decomposes the input beam into a set of plane waves (Fig. 3b). Each plane wave stimulates its own ultrasonic-reflecting sound wave. To within a first order of magnitude the power requirement from a single plane wave (attainment of threshold at the focal region) multiplied by the number of plane waves (which depends on the spatial frequency content of the modulated input beam) will give the power requirement for image retention. However, it should be realized that for a given image, not all Fourier (plane waves) components are of equal intensity. For some frequency components threshold may not be attained simultaneously with others, thus preventing high quality image retention of the SBBS beam. We thus have a limitation for image retention in SBBS of a focused beam, which does not hold in four-wave mixing.

This limitation can partially be circumvented by using tapered waveguide configurations [10-13], as originally suggested by Zel'dovich and analyzed by Hellwarth.

Experimental Demonstration of SBBS with an Ultraviolet Excimer Laser

The first demonstrations of phase conjugate reflection with excimer laser beams were carried out with KrF lasers at 2486 Å. Successful injection-locking of the KrF laser [4,6] provided in $\sim$ 1 cm coherence length ($\sim$ 50 GHz bandwidth) which was sufficient for both four-wave mixing experiments (6,7) and SBBS (the free running laser bandwidth was $\sim$ 10 Å). The nonlinear medium (liquids) which were used absorbed the ultraviolet radiation quite strongly ($\sim$ 25%/cm). For four-wave mixing experiments, this absorption was necessary for the production of thermal gratings. However, for SBBS the absorption seemed to deteriorate the reflected beam's quality. Although reflectivities higher than $\sim$ 70% were attained, the reflected beam's divergence was at least X7 the diffraction limit and the process did not reproduce itself from shot to shot.

In an effort to gain better understanding of the phase conjugation properties of stimulated Brillouin scattering and to conclusively demonstrate efficient phase conjugation in the ultraviolet, we sought to match liquids which are nonabsorbing with an ultraviolet laser of long coherence length. In particular, we have successfully demonstrated the injection locking of an XeF discharge laser using as the injection source the coincidental output of an AR^{++} laser transition at 3511 Å [5]. This laser, when used with transparent liquids with large Brillouin gains (and known acoustic decay times substantially shorter than the 30-ns laser pulse) provided an ideal situation to investigate the BSB process and demonstrated efficient ultraviolet phase conjugation.

Experimental Setup for SBBS

The experimental setup is depicted in Fig. 4. A pulsed low power (∿ 1 W) Ar-ion laser (∿ 1-GHz bandwidth) operating on the Ar-III 3511 Å transition is used to injection lock an unstable resonator XeF laser. The free-running XeF laser had a multiline bandwidth of ∿ 1 Å (500 GHz), whereas the locked XeF oscillator, described in Ref. [8], emits ∿ 60% of its energy in the 1 GHz bandwidth (coherence length ∿ 50 cm) and ∿ 40% of its energy in other unlocked transitions which are not available for locking because they originate from different upper states. The ∿ 50-mJ output (∿ 30-ns pulse duration) is in a square cross-section beam 18-mm wide with a hole (6-mm diameter) in the center. The locked radiation is polarized, whereas the remaining unlocked output is unpolarized. A detailed description of the injection-locked laser can be found in Ref. [5]. See paper paper K6 in these proceedings.

Again referring to Fig. 4, the ∿ 1-MW locked XeF laser beam is passed through a variable aperture mask (A) and a variable ND filter (ND) and is focused into a cell containing a liquid. The focal length of the focusing lens (L) is varied between 15 cm and 100 cm. A pellicle beamsplitter (BS, 8% reflectivity) directs the (phase-conjugated) beam toward a Fabry-Perot etalon with the spacing set to 0.5 cm. A corner cube retro-reflector (RR) directs the laser beam toward the same etalon. A photographic film at the focal plane of a 100-cm lens (L') can record simultaneously the spectra of the laser and the phase-conjugated beams. The 30 GHz free spectral range of the etalon and its finesse (∿ 20) provide a high enough spectral resolution (∿ 1.5 GHz) to observe the expected Brillouin frequency shift (∿ 6 GHz for Hexane).

A 0.1-Å-resolution ultraviolet grating spectrometer was used to determine whether or not the unlocked XeF output was also phase conjugated. The time histories of the laser and phase conjugated pulses were then analyzed using a fast photodiode, and the divergence and spatial quality of the beams were photographically recorded at a large distance (∿ 5m) from the liquid cell. The polarization of the phase conjugated beam was also measured.

Experimental Results

We have tried several liquids as Brillouin scatterers, the best results being obtained with hexane, isopropyl alcohol and benzene. The phase-conjugated reflectivities with these liquids were ∿ 40% of the total laser power, which corresponds to ∿ 70% of the fraction of laser power locked to the Ar-ion laser transition. These reflectivities were obtained with focal lengths of 15-50 cm (f-number between 7.5 and 25). Threshold conditions for BSBS were obtained with a 100-cm focal length lens and a 4-mm aperture in front of the laser. For these conditions ($f_{n\theta}$ ∿ 250) the intensity at the focal region was < 8 GW/cm^2 and the focal depth ($\lambda f_{n_0}^2$) was ∿ 1.8 cm.

Above threshold, the phase conjugated beams were found to be of diffraction-limited divergence. Figure 5a shows the laser energy distribution on the photographic plate located ∿ 5 m from the laser when a mask of several 4 mm holes was placed at the output of the laser. Figure 5b shows the energy distribution of the phase-conjugated beam at the same distance. Both the laser and reflected beams are diffraction limited. The spacings between the spots in Figs. 5a and 5b are different since the laser output beam was slightly divergent, and consequently the phase conjugated beam was slightly convergent, providing additional confirmation of the conjugation process.

Figures 6, 7, and 8 give some insight into the physical process of ultraviolet phase-conjugation with an XeF laser. Figure 6 shows the grating spectrogram of the laser beam (lower spectrum) and the phase conjugated beam (upper spectrum). We see that the reflected beam contains only the laser's power spectrum that is within the ∿ 1 GHz bandwidth locked to the 3511 Å Ar-ion line, indicating that the moving grating formed in the BSBS process acts as a narrowband filter. A similar filtration effect has recently been seen with degenerate four-wave mixing [14]. Thus, Fig. 6 strongly suggests that the BSBS has been produced mainly by the narrow bandwidth, polarized, locked XeF transition. An additional confirmation of this filtering process was obtained by finding that the phase conjugated beam was completely polarized (the polarization state being that of the locking Ar-ion laser). The unlocked transitions were unpolarized.

In Fig. 7 we present the high resolution (1.5 GHz) Fabry-Perot interferograms of the laser beam and the phase conjugated beam. Figure 7a shows the locked laser transition (L). In Fig. 7b there are three lines (L, B_1, B_2), which correspond to the laser transition (L), the phase conjugated beam (B_1) frequency shifted by ∿ 6 GHz (first Stoke beam) and a second-Stokes phase-conjugated beam (B_2). We believe that this second-Stokes beam arises in the following manner: the first-Stokes beam returns to the unstable resonator and enters with correct alignment (since it is a phase-conjugate

reflection). It travels "backwards" in the cavity until it reaches the paraxial region whereupon (aided by self-diffraction) it starts to work it' way back out. It then reemerges slightly amplified (since its Brillouin-shifted wavelength is still within the gain-bandwidth of the XeF medium) and subsequently undergoes BSBS in the liquid cell, accounting for the doubly-shifted light. Similar multiple-shift effects were observed by Hon [12] in Brillouin-scattering pulse-compression studies at 1.06 μm, but were first see in the early days of BSBS studies.

Figure 7c shows only a first-Stokes shift. It was obtained when a 10% transmission ND filter was placed at the output of the XeF laser. The initial output of the XeF laser was thus slightly above threshold for BSBS but the first-Stokes reflection experienced the attenuation two more times (both entering and leaving the unstable resonator) and so was below threshold upon its second arrival at the liquid cell.

Oscilloscope traces of the laser and phase-conjugated pulses are presented in Fig. 8. Figure 8a shows the normal XeF laser pulse, whereas Fig. 8b shows the laser output when the first-Stokes beam is allowed to reenter the cavity. The dip shortly after the peak is due to gain depletion caused by the first-Stokes beam which at that time is traveling backwards in the cavity. Figure 8c shows a typical phase-conjugated BSBS pulse. We believe that the earlier portion is the first-Stokes beam and that the latter portion is the doubly-shifted beam. The early termination of the first-Stokes reflection corresponds to the dip in the laser output see in Fig. 8b.

When the Brillouin cell was moved to a greater distance ($\sim$ 5m) from the laser, the first-Stokes beam returned to the laser after the gain was terminated. In this case the dip in Fig. 8b disappeared, the duration of the first-Stokes reflection increased (by $\sim$ 50% of the original width), and no second Stokes was seen.

Additionally, the effect of bulk absorption in the Brillouin liquid was examined by dissolving various absorbers in the hexane or isopropanol. Considerable degradation of the spatial quality of the phase-conjugated beam occurred by absorptions > 10%/cm at 3511 Å. The observed beam looked similar to what we have previously observed in our studies of KrF BSBS in liquids which were absorbing at 2485 Å. The mechanisms for this degradation are presently being studied.

Conclusions

We have used a 1 MW injection-locked unstable resonator XeF laser to produce efficient phase-conjugation of an ultraviolet (λ=3511 Å) beam via stimulated Brillouin scattering. Approximately 70% of the 1 GHz bandwidth XeF laser energy (locked to a reference Ar-ion trasition) was phase conjugated by focusing the laser bem into Hexane or isopropyl alcohol. Approximately 40% of the XeF laser output energy was not available for locking and was not phase conjugated. The stimulated acoustic grating in the liquid thus acted as a narrow-bandwidth filter. Both the laser beam and the 1-GHz bandwidth phase-conjugated beam were diffraction limited.

The first-Stokes retroreflected beam was able to reenter the XeF unstable resonator (to which it was automatically mode-matched by the phase-conjugation process) and to emerge slightly amplified, thus enabling the generation of a second-Stokes phase-conjugated beam. This effect demonstrates the possibility of using a stimulated acoustic grating as a phase-conjugating mirror for the cavity of a second excimer laser, enabling study of the properties of excimer laser operation when one of the mirrors is a phase conjugator [15], since the Brillouin mirror produces a frequency shift upon each reflection.

Finally, the introduction of an absorber into the Brillouin liquid caused a considerable deterioration of the reflected beam's spatial quality. This problem and the possibility of partially circumventing limitation to image retention in SBBS by using tapered waveguide configurations are presently being investigated. It is still ar open question whether or not e four-wave mixing configuration or an SBBS configuration is practically advantageous for phase conjugation . a high-power ultraviolet excimer laser beam.

References

[1] A. Yariv, IEEE J. Quant. Electron. QE-14, 650 (1978).
[2] B. J. Feldman, R. A. Fisher, S. L. Shapiro, Opt. Lett. 6, 84 (1981).
[3] M. D. Levenson, et al., J. Opt. Soc. Am. 71, 737 (1981).
[4] I. J. Bigio, M. Slatkine, Opt. Lett., Vol. 6, No. 7 (1981).
    M. Slatkine, I. J. Bigio, Conference on Lasers and Electro-Optics CLEO '81,
    post-deadline paper, Washington (1981).
[5] I. J. Bigio, M. Slatkine, to be published in Opt. Lett., (Jan. 1982).
    M. Slatkine, I. J. Bigio, Opt. Soc. of Am. Annual Meeting, Orlando, (Oct. 1981).
[6] R. G. Caro, M. C. Gower, Conference on Lasers and Electro-Optics, CLEO '81,
    post-deadline paper ThS11, Washington (1981).
[7] I. J. Bigio, B. J. Feldman, R. A. Fisher and M. Slatkine, Conference on Lasers and
    Electro-Optics, CLEO '81, post-deadline paper ThS3, Washington (1981).
[8] M. Slatkine, I. J. Bigio, B. J. Feldman, R. A. Fisher, to be published in Opt. Lett.
[9] R. Y. Chiao, C. H. Town, B. P. Stoicheff, Phys. Rev. Lett. 12, 592 (1964).
[10] B. Y. Zeldovich et al., Sov. Phys. JETP 15, 109 (1972).
[11] D. T. Hon, J. Opt. Soc. Am. 70, 635 (1980).
[12] D. T. Hon, Opt. Lett. 5, 516 (1980).
[13] R. W. Hellwarth in "Optical Phase Conjugation," edited by R. A. Fisher, Academic
    Press, Inc., N. Y., to be published.
[14] J. Nilsen, N. S. Gluck, and A. Yariv, Opt. Lett. 6, 380 (1981).
[15] J. AuYeung et al., IEEE J. Quant. Electron. QE-15, 1180 (1979).
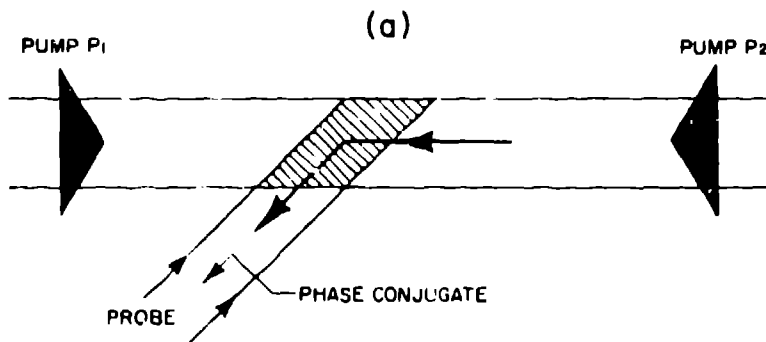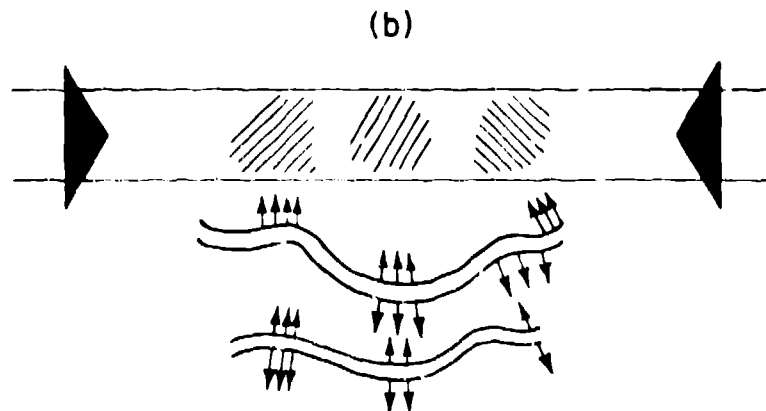
(a)

PUMP P₁   PUMP P₂

PHASE CONJUGATE

PROBE

Figure 1.

a) Schematics of phase conjugation of a probe plane wave via degenerate four-wave mixing.

(b)

b) Schematics of phase conjugation of an aberrated probe beam via degenerate four-wave mixing.
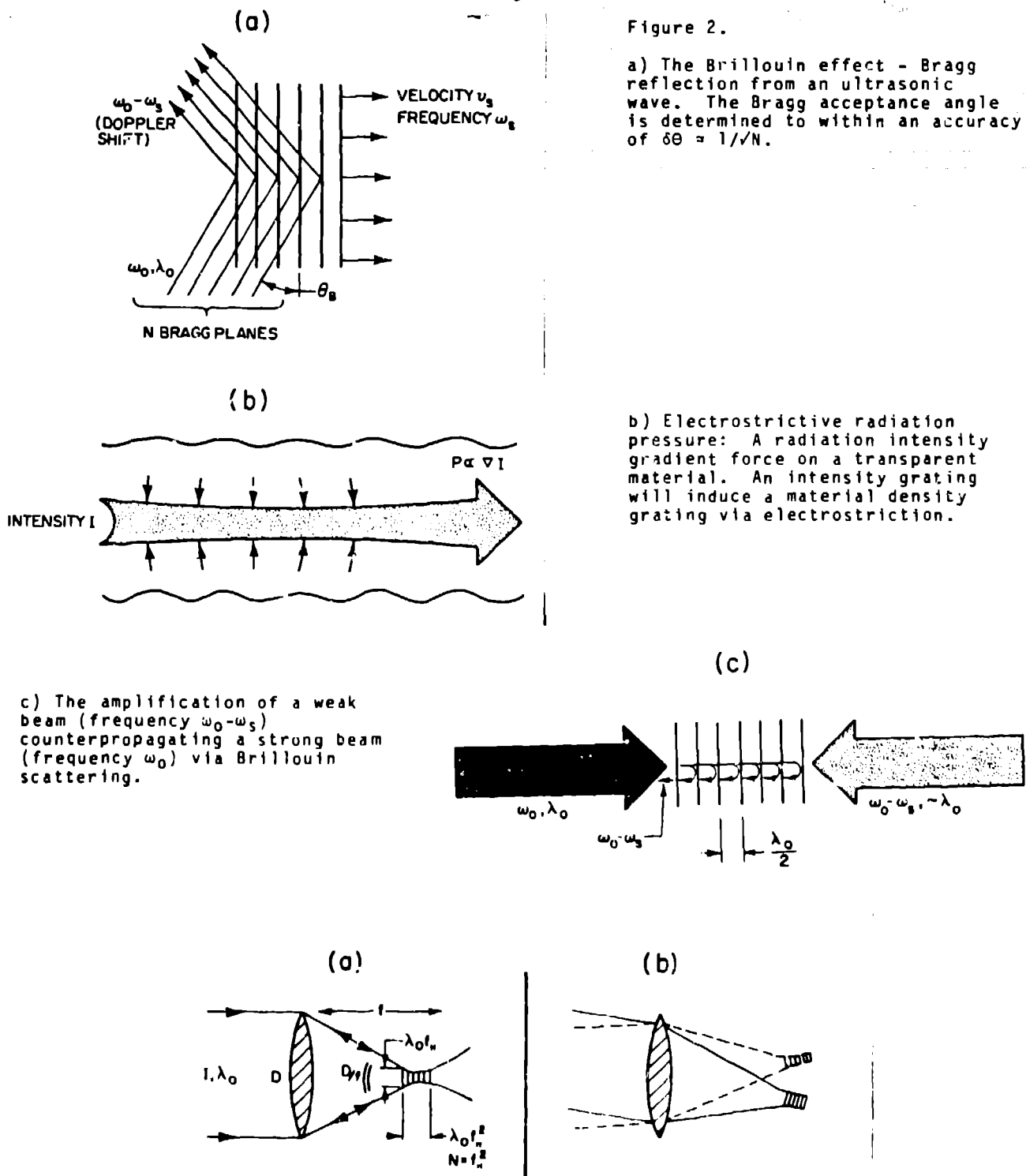
(a)

VELOCITY v_s
FREQUENCY ω_s

$\omega_0 - \omega_s$
(DOPPLER SHIFT)

ω_0, λ_0

θ_B

N BRAGG PLANES

(b)

$P \propto \nabla I$

INTENSITY I

Figure 2.

a) The Brillouin effect - Bragg reflection from an ultrasonic wave. The Bragg acceptance angle is determined to within an accuracy of $\delta\theta \simeq 1/\sqrt{N}$.

b) Electrostrictive radiation pressure: A radiation intensity gradient force on a transparent material. An intensity grating will induce a material density grating via electrostriction.

(c)

c) The amplification of a weak beam (frequency $\omega_0 - \omega_s$) counterpropagating a strong beam (frequency ω_0) via Brillouin scattering.

ω_0, λ_0

$\omega_0 - \omega_s$

$\frac{\lambda_0}{2}$

$\omega_0 - \omega_s, \sim \lambda_0$

(a)

I, λ_0 D

$\lambda_0 l_n$

$\lambda_0 l_n^2$

$N = l_n^2$

(b)

Figure 3.   a) SBBS of a focused plane wave. A small enough δ_{N_0} and a long enough coherence length are required for high-quality SBBS.

b) Image retention in SBBS can be analyzed by decomposing the spatially modulated input beam into a set of plane waves.
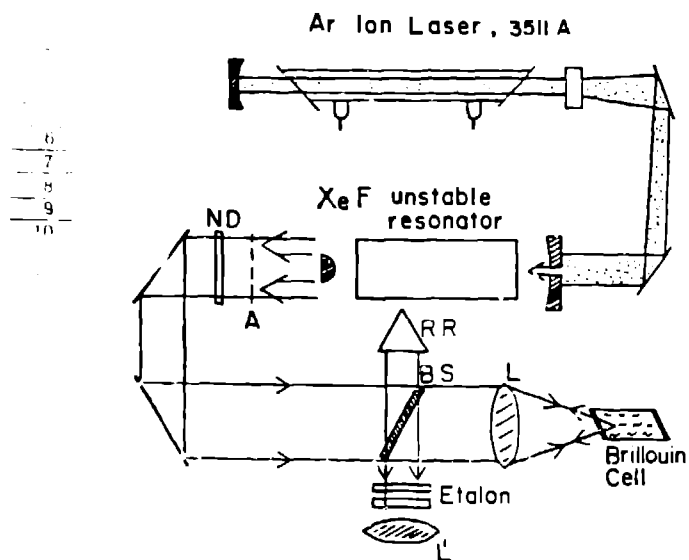
Ar Ion Laser, 3511 A

XeF unstable resonator

ND

A

R R
B S
L

Etalon

L'

Brillouin Cell

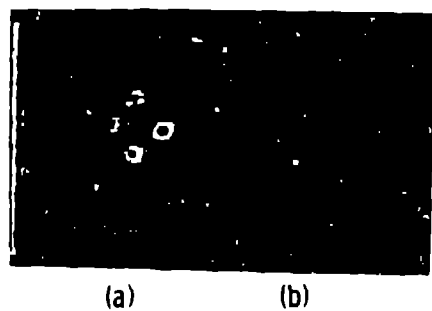Fig. 4 Experimental setup for phase conjugation of an ultraviolet XeF laser beam via stimulated Brillouin scattering.

(a)

(b)

(c)

Fig. 7. High resolution (1.5 GHz) Fabry-Perot interferograms of the laser and phase conjugated beams: a) laser beam, L; b) laser, L, and first- and second-Stokes phase-conjugated beams, B_1, B_2; c) an NDI filter has been placed at the output of the laser. Only first-Stokes is visible.

L

L
B_1
B_2

L
B_2

(a)   (b)

Fig. 5.   Intensity distribution of laser light transmitted through a mask with four 4-mm-diameter holes placed at the output of the laser: a) laser beam (slightly divergent); b) phase-conjugated beam (slightly divergent).
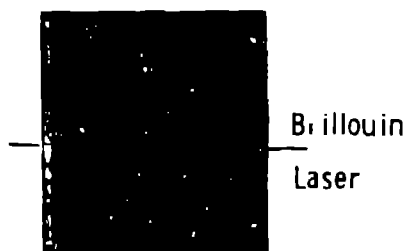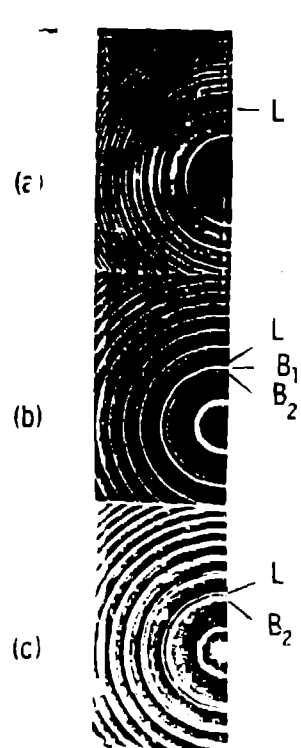
Brillouin

Laser

Fig. 6.   Grating spectrogram (0.1 Å resolution) of the injection-locked XeF laser (lower spectrum) and the phase conjugated reflection (upper spectrum).

Intensity

a
b
c

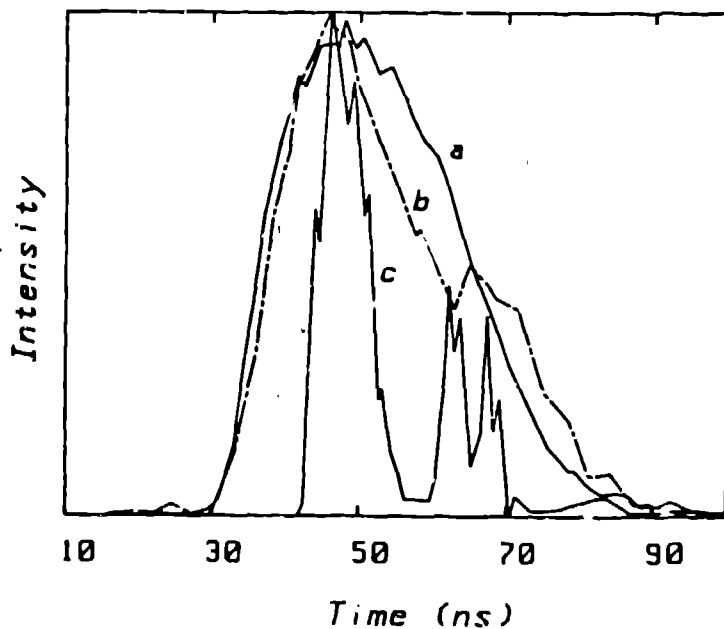10   30   50   70   90

Time (ns)

Fig. 8.   Time histories of laser and phase-conjugated pulses: a) laser pulse with no Brillouin cell; b) laser pulse showing gain depletion due to backward traveling Brillouin signals; c) first-Stokes and second-Stokes reflections.